Surfactant-Templated Silica Mesophases Formed in Water:Cosolvent Mixtures

Mark T. Anderson,*,† James E. Martin, Judy G. Odinek, and Paula P. Newcomer

Sandia National Laboratories, Albuquerque, New Mexico 87185

Received June 30, 1997. Revised Manuscript Received November 4, 1997[⊗]

Silica/surfactant mesophases have been synthesized in 14 water:cosolvent mixtures by combining tetramethoxysilane with a basic 2 wt % CTAB solution. The effects of the water-to-cosolvent ratio on the formation of supramolecular surfactant templates and ultimately silica/surfactant mesophases is reported for: diethyl ether, ethyl acetate, tetrahydrofuran, tetraglyme, methylene chloride, 2-propanol, acetone, ethanol, methanol, ethylene glycol, acetonitrile, glycerol, formamide, and *N*-methylformamide. X-ray diffraction (XRD), dynamic and static light scattering (DLS/SLS), scanning and transmission electron microscopies (SEM/TEM), and nitrogen sorption techniques are used to characterize the mesophases. Generally, polar cosolvents decrease the extent of aggregation of CTAB and lead to an evolution from ordered (o-H) hexagonally packed silica (HPS) to disordered (d-H) HPS as the cosolvent concentration is increased. Polar cosolvents allow the unit cell size of the mesophase to be tuned continuously over ∼5 Å: protic solvents decrease the cell size; aprotic solvents increase the cell size. Highly polar protic solvents, such as formamide and ethylene glycol, support substantially nonaqeous synthesis of o-H and d-H mesophases with water:silica ratio less than 4.0. Low dielectric constant cosolvents lead to expanded o-H mesophases at low concentrations, and cubic and lamellar phases at higher concentrations. Cosolvents can be used to synthesize mixed-metal framework structures from homogeneous solutions by premixing molecular inorganic precursors in a compatible nonaqueous solvent and then controllably hydrolyzing the precursors. Cosolvents also influence microstructure, leading to smaller, more curved primary particles than in pure water.

Introduction

Silica/surfactant mesophases are formed in solution by one of two complementary approaches: (1) cooperative assembly of small silicate species with micelles and individual surfactant molecules[1−7] or (2) liquid crystal templating of molecular inorganic species around a preformed, spatially extended organic superstructure.[8] In either case the resulting composite mesophases typically have a silicotropic liquid crystalline (SLC)[9] structure akin to the liquid crystalline (LC) found for surfactants in water. The three common silica/surfactant structure types are lamellar (2-d), cubic (3-d), and hexagonal (1-d),[10] which correspond to D, Q, E liquid crystalline phases.

In the absence of silica, surfactant/solvent liquid crystalline (LC) phases similar to those found in aqueous systems exist in polar nonaqueous solvents. For example, LC phases exist for the cationic surfactant cetyltrimethylammonium bromide (CTAB) in formamide,[11−15] ethylene glycol,[11,12,16] and glycerol.[11,12,14] LC phases also exist for CTAB in mixed water:alcohol systems.[17] Despite the existence of LC phases in nonaqueous solvents, there are only a few reports of the use of cosolvents in the formation of hexagonally packed silica (HPS),[6,18,19] and no systematic studies have been reported for the silica system.

* Corresponding author.
† New permanent address: Ceramic Technology Center, 3M Center, Building 201-4N-01, Saint Paul, MN 55144.
⊗ Abstract published in *Advance ACS Abstracts,* December 15, 1997.

(1) Beck, J. S.; Vartuli, J. C.; Roth, W. J.; Leonowicz, M. E.; Kresge, C. T.; Schmitt, K. D.; Chu, C. T−W.; Olson, K. H.; Sheppard, E. W.; McCullen, S. B.; Higgins, J. B.; Schlenker, J. L. *J. Am. Chem. Soc.* **1992**, *114*, 10834−10843.
(2) Kresge, C. T.; Leonowicz, M. E.; Roth, W. J.; Vartuli, J. C.; Beck, J. S. *Nature* **1992**, *359*, 710−712.
(3) Huo, Q.; Margolese, D. I.; Ciesla, U.; Feng, P.; Gier, T. E.; Sieger, P.; Leon, R.; Petroff, P. M.; Schuth, F.; Stucky, G. D. *Nature* **1994**, *24*, 317−321.
(4) Huo, Q.; Margolese, D. I.; Ciesla, U.; Demuth, D. G.; Feng, P.; Gier, T. E.; Sieger, P.; Firouzi, A.; Chmelka, B. F.; Schuth, F.; Stucky, G. D. *Chem. Mater.* **1994**, *6*, 1176−1191.
(5) Chen, C.−Y.; Li, H.−X.; Davis, M. E. *Micropor. Mater.* **1993**, *2*, 27−34.
(6) Tanev, P. T.; Pinnavaia, T. J. *Science* **1995**, *267*, 865−867.
(7) Beck, J. S.; Vartuli, J. C.; Kennedy, G. J.; Kresge, C. T.; Roth, W. J.; Schramm, S. E. *Chem. Mater.* **1994**, *6*, 1816−1821.
(8) Attard, G. S.; Glyde, J. C.; Goltner, C. G. *Nature* **1995**, *378*, 366−368.
(9) Firouzi, A.; Kumar, D.; Bull, L. M.; Besier, T.; Sieger, P.; Huo, Q.; Walker, S. A.; Zasadzinski, J. A.; Glinka, C.; Nicol, J.; Margolese, D.; Stucky, G. D.; Chmelka, B. F. *Science* **1995**, *267*, 1138.
(10) See for example; Raman, N.; Anderson, M. T.; Brinker, C. J. *Chem. Mater.* **1996**, *8(8)*, 1682−1701.
(11) Torbjöran, W.; Jönsson, A. *J. Colloid Int. Science* **1988**, *125*(2), 627−633.
(12) Auvray, X.; Perche, T.; Petipas, C.; Anthore, R.; Marti, M. J.; Rico, I.; Lattes, A. *Langmuir* **1992**, *8*, 2671−2679.
(13) Rico, I.; Lattes, A. *J. Phys. Chem.* **1986**, *90*, 5870−5872.
(14) Auvray, X.; Petipas, C.; Anthore, R.; Rico, I.; Lattes, I. *J. Phys. Chem.* **1989**, *93*, 7458−746.
(15) Perche, T.; Auvray, X.; Petipas, C.; Anthore, R.; Rico, I.; Lattes, A.; Bellissent, M. C. *J. Phys. I* **1992**, *2*, 923−942.
(16) Nagarajan, R.; Wang, C.-C. *J. Colloid Inter. Sci.* **1996**, *178*, 471−482.
(17) Fontell, K.; Khan, A.; Lindström, Maciejewska, D.; Puang-Ngern, S. *Colliod Polym. Sci.* **1991**, *269*, 727−742.

S0897-4756(97)00460-2 CCC: $15.00
Published on Web 01/19/1998

In this paper we present a systematic study of the effects of cosolvents on the formation of HPS from dilute CTAB systems that initially contain only micelles or free surfactant molecules (approach 1). Even though the HPS is formed from a "self assembly" process rather than from templating around preformed LC phases, we expect the cosolvents to affect the formation process, as, from the literature, it is well-known that nonaqueous solvents affect (1) the phase behavior of the organic amphiphile (in this case CTAB)[11−17,20,21] and (2) the inorganic chemistry of silica.[22]

It is convenient to examine the behavior of amphiphiles (without silica) in nonaqueous solvents with respect to the solvent dielectric constant. For high dielectric constant nonaqueous polar solvents, such as formamide,[11−15] ethylene glycol,[11,12,16] glycerol,[11,12,14] and *N*-methylformamide,[11,12] conventional ionic surfactants such as CTAB can associate to form LC phases. It is thus expected that, in these highly polar solvents, formation of SLC HPS may occur similarly as in a purely aqueous environment. Several important differences in phase behavior are noted between aqueous and nonaqueous solvents. In general, the amphiphiles form LC phases much less readily in nonaqueous solvents than in water.[11] For example, with formamide CTAB forms premicellar aggregates (as few as 6 molecules per aggregate) in dilute systems[15] and eventually micelles at higher concentrations. The micelles in formamide have smaller diameters and aggregation numbers than in water.[15] The existence regions of LC phases with respect to temperature and concentration are smaller in polar nonaqueous solvents than in water,[11] and follow the order: water > formamide ≫ glycerol > ethylene glycol > *N*-methylformamide. This sequence follows the decrease in interfacial tension between solvent and hydrocarbon (dodecane).[11]

For intermediate dielectric constant solvents such as methanol, ethanol, 2-propanol, acetone, the methanol, the water/alcohol/CTAB (alcohol is methanol and ethanol) systems have been studied in detail.[17] In both cases only isotropic L and hexagonal E phases exist.[17] Increasing the alcohol-to-water ratio decreases the average aggregate diameter and increases the area per headgroup for the surfactant,[17] which means that some control over the template size should be possible in HPS synthesis, depending on the alcohol concentration.

For relatively low dielectric constant solvents in low concentrations, it is convenient to view them as additives that can solubilized in the micellar structure owing to their considerable hydrophobicity.[20] The less polar and more branched the solvent, the deeper it is solubilized in the micelle. Molecules solubilized deep within the micelle can be expected to swell the micelle and increase the propensity for the formation of lamellar phases.[23,24]

In general, polar molecules, in addition to residing in the continuous phase, can be dissolved into the micelles. Polar and polarizable solubilizates are thought to be distributed between adsorbed state at the micelle-water interface and dissolved state in the hydrocarbon core.[20] Small polar molecules in aqueous medium are generally solubilized close to the surface in the palisade layer or by adsorption at the micelle−water interface.[20] The locus of solubilization of any solubilizate, polar or nonpolar, influences the size and shape of the template, and ultimately the pore diameter and structure of silica/surfactant mesophases.

Nonaqueous cosolvents are expected to affect the inorganic chemistry of silica,[22] as well as the phase behavior of CTAB. It must be kept in mind that, although we discussed some purely nonaqueous systems above, the presence of some water is necessary in the preparation of HPS to hydrolyze the silica source tetramethoxysilane (TMOS). TMOS is a hydrophobic molecular silica source and is initially immiscible with water.[25] The cosolvents are expected to affect the initial solubility of the TMOS in the solvent. For example, TMOS is readily soluble in pure methanol, ethanol, and acetonitrile and is solubilized about five times faster in formamide than in water (this work). The cosolvents are also expected to affect the kinetics of TMOS hydrolysis and condensation as well as its speciation depending on their polarity, dipole moment, and availability of labile protons.[22]

Three reactions can generally be used to describe the progression of silicate chemistry[22] (sol−gel process) for alkoxides in water:

$$\equiv Si{-}OR + H_2O \leftrightarrow \equiv Si{-}OH + ROH \qquad (1)$$

(forward: hydrolysis; reverse: esterification)

$$\equiv Si{-}OR + HO{-}Si\equiv \leftrightarrow \equiv Si{-}O{-}Si\equiv + ROH \qquad (2)$$

(forward: alcohol condensation; reverse: alcoholysis)

$$\equiv Si{-}OH + HO{-}Si\equiv \leftrightarrow \equiv Si{-}O{-}Si\equiv + H_2O \qquad (3)$$

(forward: water condensation; reverse: hydrolysis)

With respect of solvent effects on the above reactions, the availability of labile protons is especially important as it determines whether anions or cations are solvated more strongly through hydrogen bonding. This is important for base-catalyzed reactions, as the hydroxide ions and the silicate species are charged. Solvent molecules that hydrogen bond to hydroxyl ions reduce the catalytic activity under basic conditions, as they reduce their nucleophilicity. This may be expected to slow the base-catalyzed formation of small charged oligomers, which are believed necessary to form HPS.[9] Protic solvents are also found to retard base-catalyzed condensation, as they hydrogen bond to nucleophilic deprotonated silanols. This should have little effect on the formation kinetics of HPS, as little or no framework condensation is necessary as long as small oligomeric species are present in solution.[9]

(18) Kim, A. Y.; Liu, J.; Virden, J. W.; Bunker, B. *Materials Research Society Symposium Proceedings*; Komarneni, S.; Smith, D.; Beck, J. S. Eds.; MRS Symposium Series 371; Materials Research Society: Pittsburgh, PA, 1995; pp 105−110.
(19) Vaudry, F.; Khodabandeh, S.; Davis, M. E. *Chem. Mater.* **1996**, *8*, 1451−1464.
(20) Rosen, M. J. *Surfactants and Interfacial Phenomena*; Wiley: New York, 1989; Chapters 3 and 4.
(21) Meyers, D. *Surfactant Science and Technology*; VCH: New York, 1992; Chapters 3 and 4.
(22) Brinker, C. J.; Scherer, G. W. *Sol−Gel Science*; Academic: New York, 1990.
(23) Beck, J. S. US Patent 5,057,296, 1991.
(24) Monnier, A.; Schuth, F.; Huo, Q.; Kumar, D.; Margolese, D. I.; Maxwell, R. S.; Stucky, G. D.; Krishnamurty, M.; Petroff, P.; Firouzi, A.; Janicke, M.; Chmelka, B. F. *Science* **1993**, *261*, 1299−1303.
(25) Cogan, J. D.; Setterstrom, C. A. *Chem., Eng. News* **1946**, *24*, 2499.

Table 1. Physical Properties of Cosolvents

cosolvent	formula	polar	protic	donor	ϵ (25 °C)[a]	o-H →[b]
ether	$H_5C_2OC_2H_5$			x	4.3	C, L
ethyl acetate	$CH_3C{=}OOC_2H_5$			x	6.0	d-H
tetrahydrofuran	C_4H_4O			x	7.6	L
tetraglyme	$CH_3(OCH_2CH_2)_4OCH_3$			x	7.7	d-H
methylene chloride	H_2CCl_2				8.9	L
2-isopropanol	C_3H_7OH	x	x	x	18	d-H
acetone	$CH_3C{=}OCH_3$	x		x	21	d-H
ethanol	C_2H_5OH	x	x	x	24	d-H
methanol	CH_3OH	x	x	x	33	d-H
ethylene glycol	$C_2H_6O_2$	x	x	x	37	d-H
acetonitrile	$CH_3C{\equiv}N$	x		x	38	d-H
glycerol	$CH_2OHCHOHCH_2OH$	x	x	x	43	d-H
water	H_2O	x	x	x	78	d-H
formamide	$HC{=}ONH_2$	x	x	x	111	d-H
N-methylformamide	$HC{=}ONHCH_3$	x	x	x	188	d-H

[a] e = dielectric constant. [b] o-H → indicates structural evolution with increased cosolvent concentration.

Here we present the effects of cosolvents on the micellization of surfactant templates, and the formation, structure, long-range structural ordering, kinetics, cell constant, and porosity of surfactant-templated silica mesophases. We chose a variety of cosolvents with differing polarities, hydrogen bonding abilities, and electron-donating abilities to investigate the effects of these properties on mesophase formation. We find that the polarity of the cosolvent generally affects the (1) critical micelle concentration of the surfactant, reducing it for polar cosolvents, (2) the existence region of ordered HPS, which is much larger for polar than nonpolar cosolvents, (3) the structural evolution of silica surfactant mesophases: polar solvents lead from o-H to d-H as their concentration increases, whereas nonpolar solvent lead from o-H to C or L as their concentration increases, (4) the ability to perform syntheses under substantially nonaqueous conditions; highly polar protic solvents allow synthesis of HPS where water is essentially just a reagent (water:Si as low as ∼4). The hydrogen bonding ability of the cosolvents affects the ability to tune the cell constant of the resulting mesophases: protic solvents lead to a decrease in unit cell, whereas aprotic solvent increase the cell constant. Generally, the cosolvents have little effect on the overall formation kinetics of HPS, except where the systems assemble from free, rather than micellized, surfactant.

Experimental Section

1. Synthesis. We synthesized silica/surfactant mesophases from 14 water:cosolvent mixtures. A typical synthesis involved mixing 9.8 g deionized water plus cosolvent (usually 100:0 90:10 ... 10:90 w/w), 0.2 g (0.55 mmol) of cetyltrimethylammonium bromide, (CTAB; Fisher, 99+%), 0.065 mL of 50 wt % NaOH (1.14 mmol), and 0.625 mL (4.23 mmol) of tetramethoxysilane (TMOS, United Chemical Technologies). The molar ratios of silica, surfactant, and base were kept constant at 1 TMOS: 0.13 CTAB: 0.29 NaOH. Water-to-silicon ratios varied from 129:1 to < 4:1, depending on the water-to-cosolvent ratio.

A variety of simple ethers, esters, carboxylic acids, glycols, ketones, amides, nitriles, and alcohols were used as cosolvents, Table 1. These include polar and nonpolar, protic and aprotic, donating and nondonating solvents. The Krafft temperatures for CTAB are higher in some solvents than in water, so some of the mixtures had to be heated to about 50 °C to dissolve the surfactant (e.g. T_{Krafft} in formamide is 43 °C and in water is 26 °C).[13]

To prepare the mesophases a basic micellar solution was prepared, and then TMOS was added. Adding the TMOS to the precursor solutions resulted in weak particulate gels. After aging (1 min to 30 days) at room temperature, the wet silica/surfactant gels were suction filtered, washed with deionized water, and dried in air. The surfactant typically was removed from the product by calcination. The calcination process involved a linear temperature ramp from 25 to 550 °C over 2−10 h in flowing N_2; an isotherm at 550 °C for 1−2 h; cooling to <300 °C; a linear ramp to 550 °C in flowing O_2; an isotherm for 6−10 h; and cooling to room temperature in flowing oxygen (furnace off).

2. X-ray Diffraction. Data were collected with a Scintag PAD V instrument using nickel-filtered Cu K_α radiation. Data were collected in continuous scan mode from 1.5 to 10° 2θ with a 0.02° sampling interval and a 1°/min scan rate. Slits widths starting from the source were 1, 2, 1, and 0.3 mm. Tube voltage was 45 kV and tube current was 35 mA. Peak positions and full-widths at half-maxima were determined with Scintag analysis software (TC9 package). Peak positions for the periodic hexagonal phase were corrected with an external standard routine. The routine used four Bragg peaks (*100, 110, 200, 210*) for the correction. Linear least-squares analysis of the peak positions yielded accurate lattice parameters.

3. Light Scattering. Dynamic and static light scattering measurements were made with a 63 mW NEC He−Ne laser, using a 256 channel Langley-Ford correlator. A Malvern index-matching temperature-controlled scattering vat, a Malvern detector assembly, using an RCA FW130 photomultiplier tube, and an Aerotech 12 in. stepper-motor-driven goniometer complete the basic light scattering hardware. The system is automated by a DEC PDP-11/73b computer.

Intensity autocorrelation functions were fit to single exponential decays, and the micelle radius was determined from the heterodyne decay rate Γ from the standard relation $\Gamma = D_t q^2$ where q is the scattering wavevector and D_t is the translational diffusion constant. The Stokes−Einstein relation $D_t = k_B T/6\pi\eta R$ was then used to extract the radius.

The static intensity data were taken on the same instrument using a statistical procedure to discard anomalously high intensity readings due to dust. Filtration of all micelle samples in a clean bench reduced dust contamination.

4. SEM/TEM. A JEOL 1200EX transmission electron microscope (TEM) with ASID (SEM) attachment was used to observe the microstructure and grain size of the powder samples. To observe individual grains, the aggregated powders were ground under methanol in a mortar and pestle. The suspended powder was caught on the holey carbon film of a 3 mm copper grid. Bright field TEM or diffraction contrast imaging was done at 120 kV and involved low (20k times) and high (300k times) magnifications of the individual grains and small aggregates. SEM micrographs were obtained that reveled the morphology of powder aggregates and the size of the grains.

5. Gas Adsorption. A Micromeritics ASAP 2010 was used to collect N_2 sorption data at 77 K. Samples were degassed overnight at 200 °C. BET analyses were performed to deter-

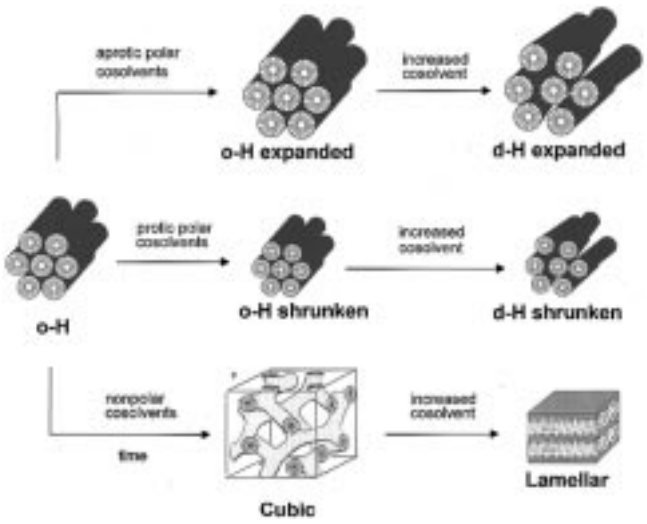

Figure 1. Summary of the effect of cosolvents on the structure, pore diameter, and periodicity of silica mesophases. (Note: o-H, ordered hexagonal; d-H, disordered hexagonal; amorphous products result at very high cosolvent concentrations.)

mine the apparent surface areas. Pore diameters were determined by application of the Kelvin Equation to the desorption branch of the data.

Results

1. Structural Evolution of Silica/Surfactant Mesophases. In water:cosolvent systems we find that five types of silica/surfactant products can be formed (Figure 1). These materials are characterized by their X-ray diffraction patterns: (1) ordered hexagonal mesophases (o-H) that exhibit at least three low angle diffraction peaks (indexed as the *100*, *110*, and *200* on a 2-d hexagonal net), (2) disordered mesophase structures (d-H) that exhibit only one (*100*) or two (*100*, *110*+*200*) diffraction peaks and have a disordered arrangement of cylindrical 1-d pores (*quasi*-hexagonal),[26,27] (3) cubic mesophase structures (C) that exhibit peaks that can be indexed with *Ia*3*d* space group symmetry,[1,2] (4) lamellar mesophase structures (L) characterized by a family of 00*l* diffraction peaks, and (5) amorphous silica (A), which exhibit no low-angle Bragg peaks.

For the pure water solvent system, $r = 0\%$ ($r \equiv$ weight percent cosolvent in the micellar solution), o-H forms. As the concentration of cosolvent is increased in any system, the structure changes from o-H to either d-H, C, or L, as shown in Figure 1 and Table 1.

The transformation from o-H to d-H for the formamide system as the concentration is increased is shown in Figure 2. The breadth of the *110* and *200* peaks increase at high concentration until it is difficult to discern their presence. Figure 2 shows an expansion of the region from $r = 84\%$ to $r = 96\%$. It is apparent that for $r = 96\%$ there are no longer two distinct peaks between 4 and 5.5° 2θ, which signals that the structure is d-H rather than o-H. Previous work by us[26] and others[27] have established that the d-H structure consists

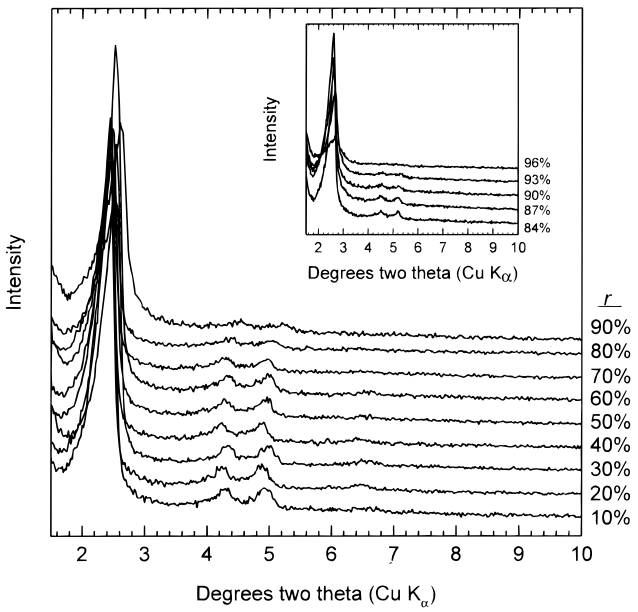

Figure 2. X-ray diffraction spectra for the water:methanol system show the evolution from o-H to d-H at $r \gg 60\%$. Note the shift of the diffraction peaks to higher values of 2q as *r* increases, which implies the cell constant decreases as *r* increases. The samples were aged 1 day. Inset shows the change from o-H to d-H at $r \gg 93\%$.

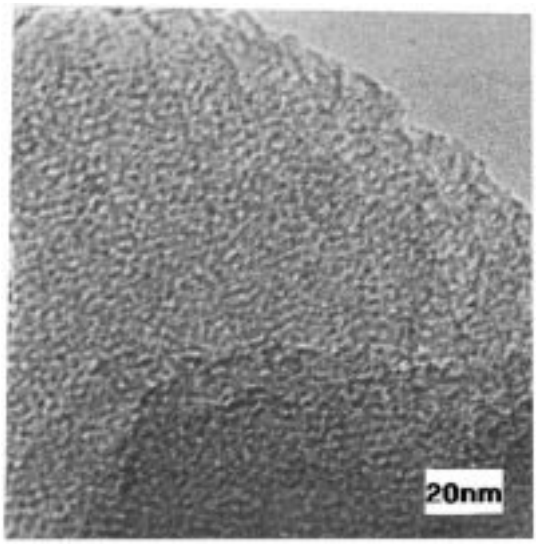

Figure 3. High-resolution transmission electron microscope (HRTEM) image of a d-H $r = 70\%$ methanol preparation. The X-ray diffraction pattern of the material exhibits only one broad peak at ~35 Å.

of disordered unimodal channels that are intergrown and intersecting. A HRTEM image of a d-H $r = 70\%$ methanol sample is shown in Figure 3. The o-H to d-H structural evolution is exhibited by ethyl acetate, tetraglyme, 2-propanol, acetone, ethanol, methanol, ethylene glycol, formamide, and *N*-methylformamide, as noted in Table 1.

The o-H to L change that occurs in the tetrahydrofuran system is illustrated in Figure 4. The system forms a well-defined lamellar phase from $r = 20-30\%$. At $r = 40\%$ what appears to be a disordered phase reappears, as evidenced by the very broad peak less than 2° 2θ. It should be pointed out that the solubility of the THF in water in this alkaline micellar system is

(26) Anderson, M. T.; Martin, J. E.; Odinek, J.; Newcomer, P. *Chem. Mater.*, submitted.
(27) Ryoo, R.; Kim, J. M.; Ko, C. H., Shin, C. H. *J. Phys. Chem.* **1996**, *100*, 17718−17721.

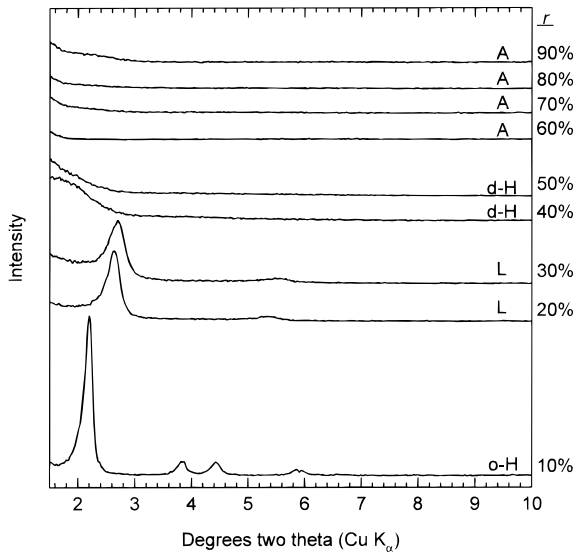

Figure 4. X-ray diffraction spectra for the water:tetrahydrofuran system show the evolution from o-H to L to d-H to amorphous as *r* increases. The samples were aged 4 days. Note that the solvent phase separates at $r > 25\%$.

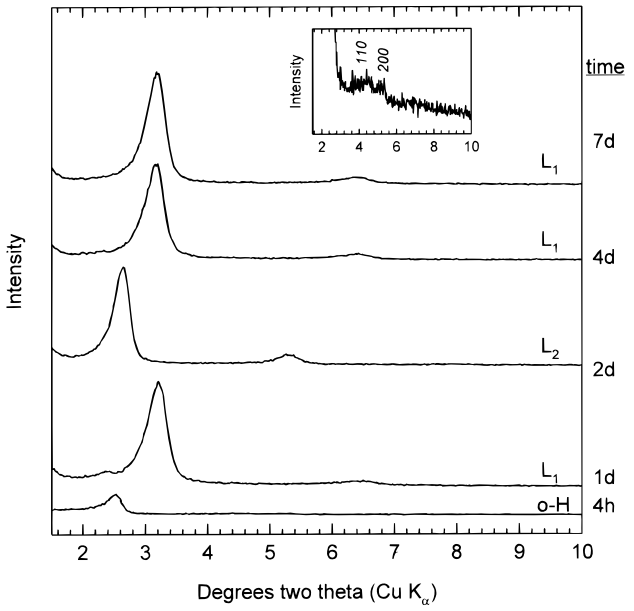

Figure 5. X-ray diffraction spectra of an $r = 20\%$ tetrahydrofuran sample aged at 60 °C show the complete transformation from o-H to lamellar (L_1) over the course of 1 d. The L_1 phase transforms to an L_2 phase with a larger cell constant and then back to the L_1 phase over the period of 2d. Inset shows the o-H phase.

exceeded at this point and the system is phase separated prior to the addition of TMOS. d-H phases can reappear in the phase-separated solvent systems. Finally, the system forms amorphous silica for $r \geq 60\%$.

The dramatic effect that aging the wet gel has on the structural transformation is presented in Figure 5. At $r = 20\%$ the structure is initially d-H. After aging at 60 °C the structure transforms from d-H to L. For longer aging times the cell constant increases (L_2) and then decrease back to approximately the value after 1 day of aging (L_1). The change in cell constants may be related to the yellow discoloration of the sample over several days, which is likely due to decomposition of some of the surfactant. If the decomposed surfactant

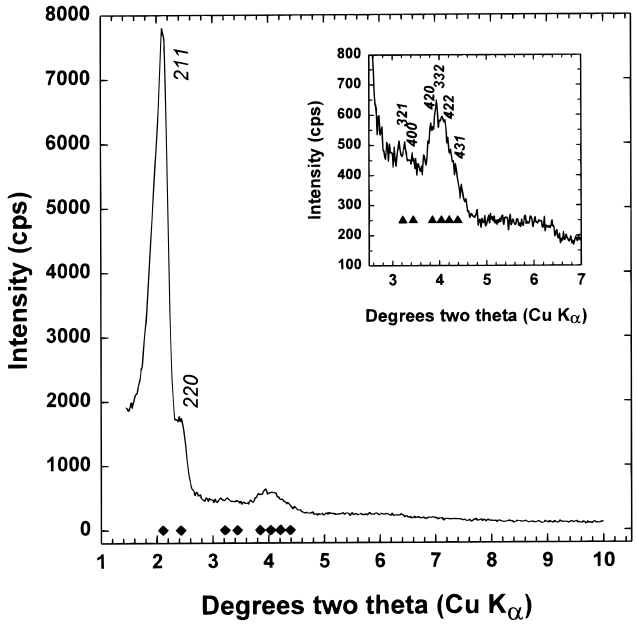

Figure 6. X-ray diffraction spectra show the poorly ordered *Ia*3*d* cubic phase that forms for $r = 10\%$ with diethyl ether. The sample was aged 5 d at room temperature. The cell constant is 102.5(5) Å as determined from the *211* and *220* reflections; the positions of the higher order reflections were generated using this cell constant and the indexing from the literature (ref 2).

swells the hydrophobic volume inside the tubular surfactant assemblies and is expelled into the continuous phase, then the expansion and contraction of the unit cell is explained. The same evolution is seen on approximately the same time scale for samples aged at 25 °C, except that the transformation from d-H is only about 80−90% complete (not shown). The d-H to L phase evolution is observed for tetrahydrofuran and methylene chloride. Figure 6 shows that a poorly ordered *Ia*3*d* cubic phase[1,2] is formed by aging in diethyl ether. The phase forms at *r* values ($r = 10\%$) between those for o-H and L.

Figure 7 shows that cosolvents can be mixed to improve the order of o-H phases. Note the better resolution of the *110* and *200* reflections for $r = 90\%$ in this figure as compared to pure formamide at $r = 90\%$ in Figure 2, and, note that the maximum value of *r* for which o-H can be formed with tetraglyme is only 70%.

The existence regions of o-H phases in all of the water:cosolvent systems studied here is summarized in Figure 8.

2. Micellization in Water:Cosolvent Mixtures. Figure 9 shows static light scattering measurements for eight different solvent systems. The scattered intensity above background increases with *r* for all the cosolvents and mixtures, which indicates a decrease in extent of aggregation or aggregate size.

3. Metrical and Porosity Data. Figure 10 shows that as the methanol concentration increases in the micellar system the hydrodynamic radius of the supramolecular aggregates decreases. There is a concomitant decrease in the unit cell parameter over this same range.

A plot of *da*/*dr* versus dielectric constant is shown Figure 11. The values of *da*/*dr* were determined from unit cell versus weight percent cosolvent plots analogous

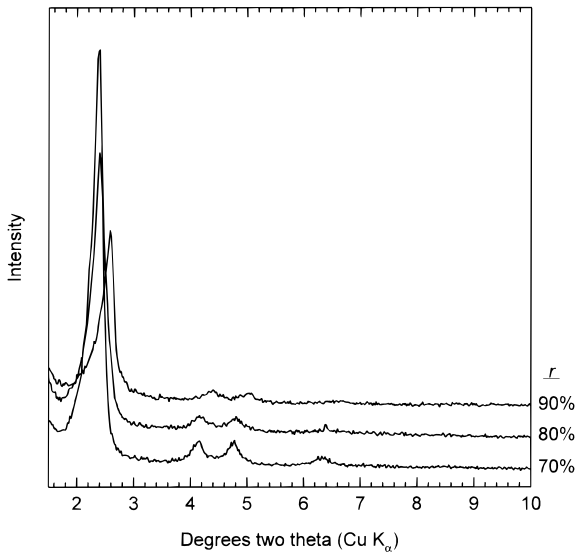

Figure 7. X-ray diffraction spectra for the water:(75:25 formamide:tetraglyme) system show that o-H products can be made at $r = 90\%$. The samples were aged 4 days.

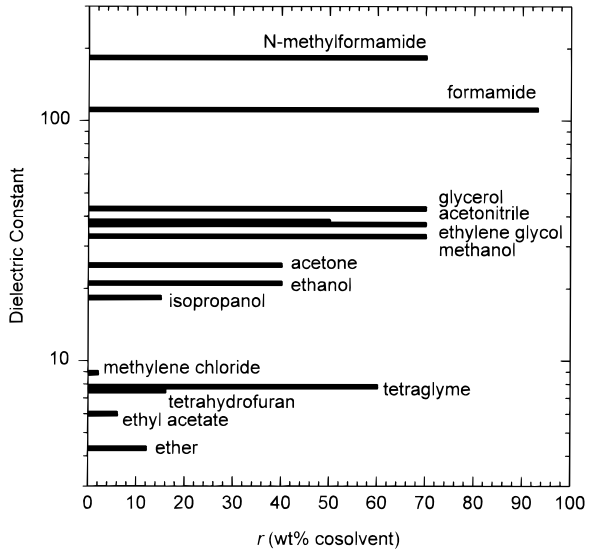

Figure 8. The Ordered Hexagonal Existence Region (o-HER) is shown for 14 cosolvents.

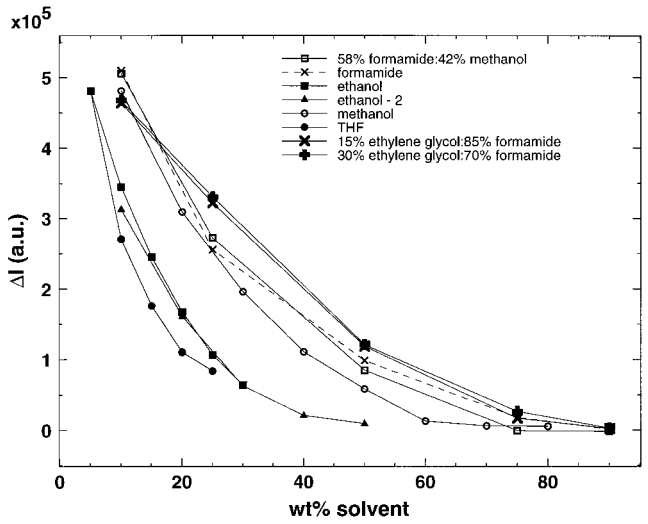

Figure 9. Static light scattering show that the intensity above background varies widely for a variety of cosolvents. The *cmc* = 0% where the differential scattered intensity is zero. Note that generally the *cmc* increases as the dielectric constant of the cosolvent increases.

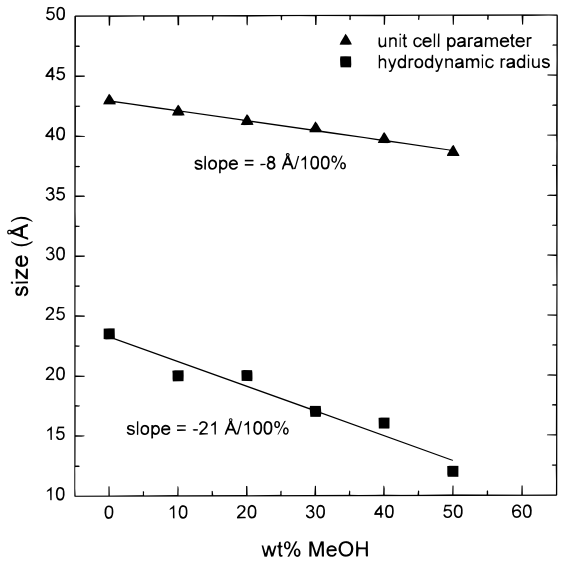

Figure 10. The cell constants of the o-H mesophases made from a water:methanol system decreases as *r* increases as do the hydrodynamic radii of micelles in the precursor solution. The slope of the *da*/*dr* plot (where *a* is cell parameter and *r* is wt % methanol) implies that if a product could be made with 100% methanol the cell constant would be 8 Å smaller than the material made with 100% water.

to that shown in Figure 10. Note that a positive value of *da*/d*r* implies that the unit cell increases with cosolvent concentration. In addition to changing the unit cell constant by varying the concentration of cosolvent, Figure 12 shows that the unit cell constant can be increased by the aging wet gels in a water/cosolvent mixture.

Figure 13 shows that an $r = 90\%$ formamide o-H sample retains periodic mesoporosity after calcination. The increase in the scattered intensity for the calcined material results from the increase in scattering contrast (uncalcined: silica framework versus template; calcined: silica framework versus air). Figure 14 confirms that the mesoporosity still exists and that the pores are accessible. There is a noticeable hysteresis in the 0.4−0.8 relative pressure region, presumably owing to capillary condensation and evaporation of the liquid nitrogen in the pores. Four-point BET analysis indicates the surface area is 550 ± 6 m^2/g, the pore volume for $P/P_o < 0.9$ is 0.47, and the BJH desorption dV/dR pore volume plot reveals a maximum at a pore diameter of 34 Å.

4. Mixed-Metal Frameworks. X-ray diffraction of SiO_2:Al mesophases is presented in Figure 15. The mixed framework materials are formed by premixing the silica and alumina sources in 2-propanol to form a homogeneous solution. This mixed-metal solution is added to the alkaline micellar solution, and after 7−10 s an aluminum-containing periodic mesophase gel results. The FWHM of the *100* reflection is a minimum for the $r = 5\%$ sample, which indicates that it has the longest range order of the 2-d hexagonal net. Figure 16 shows the ^{27}Al NMR from the uncalcined $r = 5\%$ sample. The single resonance indicates that all of the detectable aluminum is 4-coordinate. The spectra for

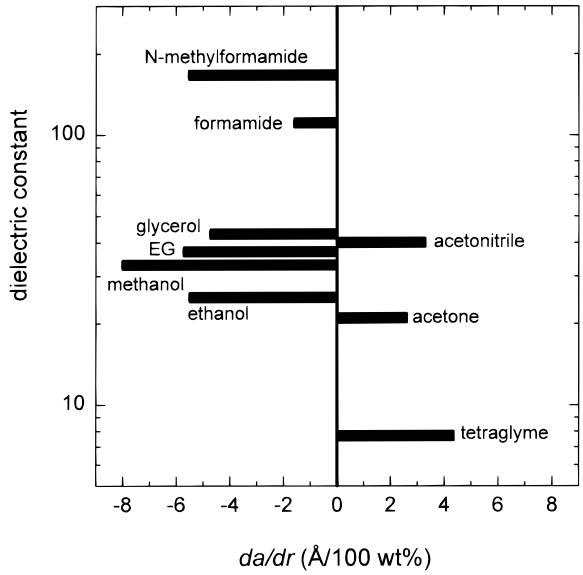

Figure 11. The graph shows *da*/*dr* (see Figure 10) for the cosolvents indicated. *da*/*dr* is simply the slope of the cell constant (*a*) versus weight percent cosolvent (*r*) plot. A negative value indicates the cell constant decreases with an increase in *r*.

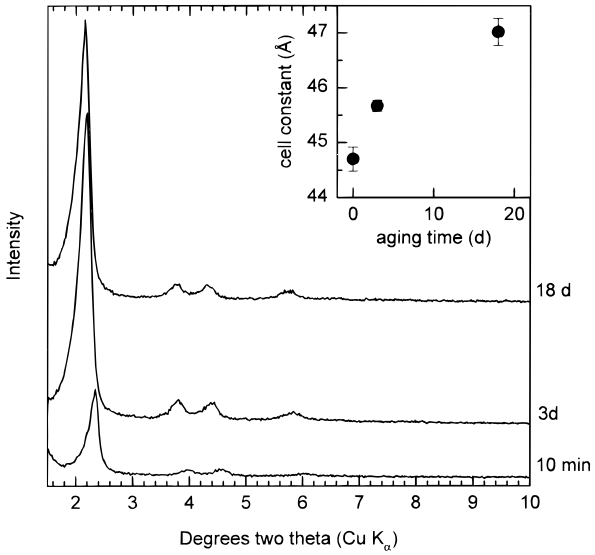

Figure 12. The increase in cell parameter with aging time seen for the water:methylene chloride system is consistent with slow decomposition of surfactant within, or imbibition of cosolvent into the hydrophobic interior of the surfactant arrays, or a combination of the two as the surfactant array structure changes over time. The regularity of the 2-d array of pores is not affected by the long aging time, as indicated by the retention of four diffraction peaks.

the other four sample are virtually identical. After calcination approximately 2/3 of the Al is 4-coordinate. The rest is 5- or 6-coordinate and is assumed to be extraframework, which occurs commonly for mixed-metal Al:SiO_2 framework mesophases.[5,28,29]

5. Microstructure. The effect that cosolvents have on microstructure is shown in Figure 17.

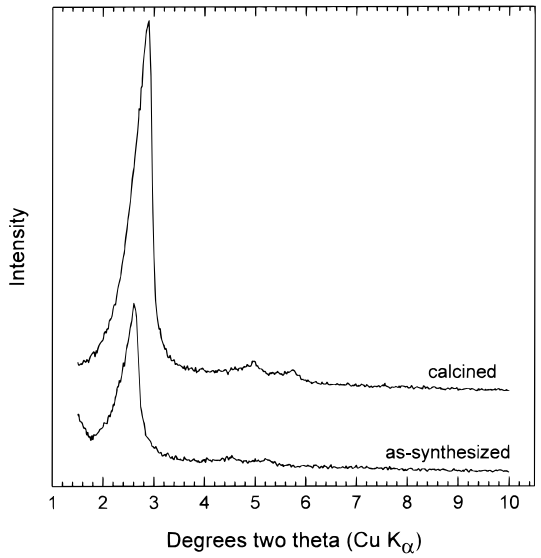

Figure 13. X-ray diffraction spectra of an as-made and calcined $r = 90\%$ formamide sample. The calcined sample exhibits three peaks, which indicates it retains its ordered hexagonal arrangement of pores. The cell constant shrinks ~8.5% owing primarily to the condensation of framework silanol groups at high temperature.

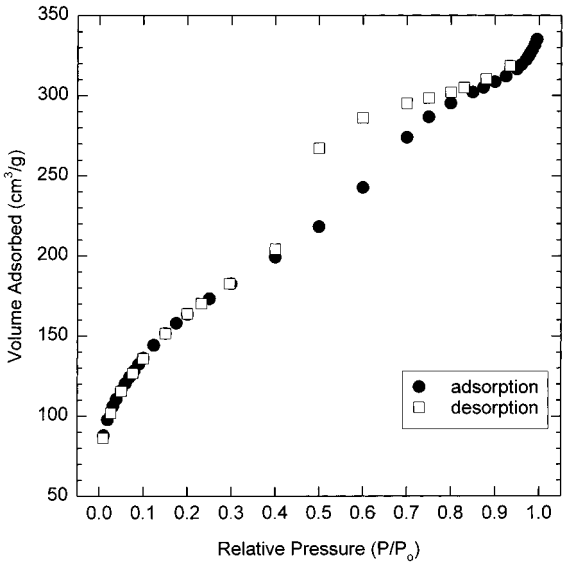

Figure 14. N_2 sorption isotherm collected at 77 K on the $r = 90\%$ formamide sample shown in Figure 13.

Discussion

1. Micellization and Template Size in Water: Cosolvent Systems. We first review the behavior of CTAB in water to put its behavior in cosolvents in context. In purely aqueous systems CTAB[30] has a *cmc* of $\sim 9.9 \times 10^{-4}$ M at 25 °C. For concentrations above *cmc*, CTAB forms more or less spherical, strongly hydrated micelles (hydration number 9 ± 3)[31] composed of about 90−95 molecules;[32] above 9−11 wt% the sperhical micelles are deformed to rod-shaped shaped micelles;[32] above 26 wt % the isotropic micellar solution

(28) Schmidt, R.; Akporiaye, D.; Stocker, M.; Ellestad, O. E. *J. Chem. Soc., Chem. Commun.* **1994**, 1493.
(29) Corma, A.; Fornes, V.; Navarro, M. T.; Perez-Pariente, J. *J. Catal.* **1994**, *148*, 569.
(30) Lawrence, A. S. C.; Stenson, R. Proc. Int. Congr. Surf. Act. *2nd*, 1957, II, 368.
(31) Coppola, L.; Muzzalupo, R.; Ranieri, G. A.; Terenzi, M. *J. Phys. II* **1994**, *4*, 2127−2138.
(32) Ekwall, P.; Mandell, L.; Solyom, P. *J. Colloid Inter. Sci.* **1971**, *35(4)*, 519−528.

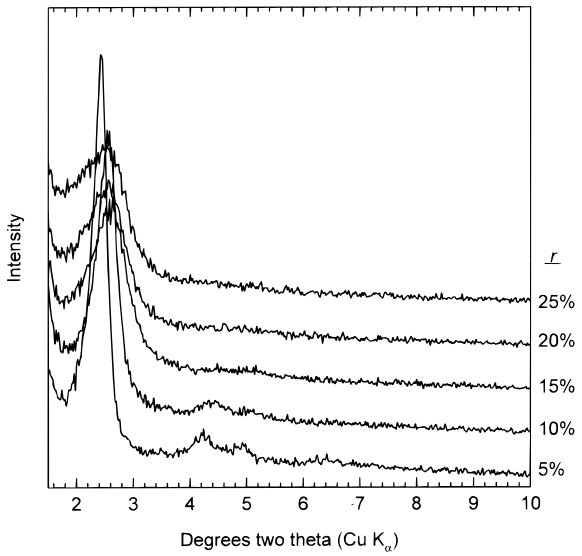

Figure 15. X-ray diffraction spectra from samples made by premixing TMOS and Al(*sec*-OBu)$_3$ in a 10:1 molar ratio in 2-propanol and then adding this solution to an aqueous alkaline micellar solution. The value of *r* indicates the weight percent 2-propanol in the final mixture.

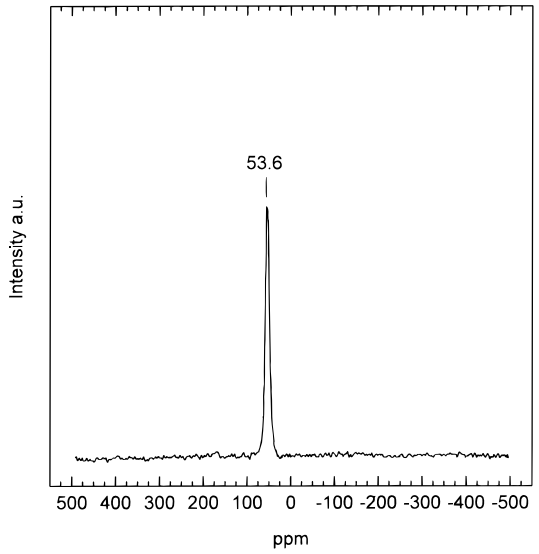

Figure 16. ^{27}Al solid-state magic angle spinning NMR recorded on the $r = 5\%$ sample indicate all of the Al is four coordinate.

(L) is transformed to LC phases, in order, a hexagonal phase (E), a cubic (Q) phase, and a lamellar (D) phase.[32]

The observed decreases in scattered intensity above background with increasing cosolvent concentration measured in SLS for methanol,[17] ethanol,[17] and formamide[11−15] (Figure 9) are expected from the literature, as aggregation is disfavored in the pure solvents. Specifically, for the formamide system, the *cmc* of CTAB[12] is about 2.8 wt % ($\sim 8 \times 10^{-2}$ M) for small, highly charged 6 monomer premicellar aggregates[15] and 8−9 wt % for 30 monomer micelles at 60 °C.[15] Thus, the *cmc* is about 2 orders of magnitude higher in formamide than in water. The increased *cmc* in pure formamide has been attributed to the reduced solvophobic interactions of the alkyl tail with formamide as opposed to water.[12] As we approach $r = 100\%$ formamide in the mixed solvent system, we expect *cmc* to exceed the nominal 2 wt % used in all the experiments reported here. We see evidence of that the *cmc* exceeds 2 wt % at $r = 90\%$, as the scattered light intensity above background is zero as measured by SLS (Figure 9). In addition to the much greater *cmc* of formamide as compared to water, the micelles in water elongate at concentrations below the L → E boundary, whereas those for formamide only begin to elongate near the E → Q boundry.[14]

The behavior of ethylene glycol[11,12,16] is, overall, very similar to formamide based on literature reports. Note that *cmc* of CTAB in ethylene glycol is comparable to that of formamide at about 1.4×10^{-1} M at 60 °C.[12]

For the methanol and ethanol systems, the decrease in scattering intensity is consistent with a decrease in *cmc* also.[26] The decrease in *cmc* is expected from the literature, as aggregation is disfavored in these alcoholic systems. Evidence of decreased favorability of aggregates is the penetration of the simple isotropic L phase into the center of the water:alcohol:CTAB ternary phase diagram[17] and the absence of Q and D phases in the ternary alcoholic systems.

The decrease in micellar size (Figure 10) detected with dynamic light scattering as the methanol:water ratio is increased is analogous to the reported reduction in unit cell size for the E phase at 55 wt % CTAB as the ethanol concentration in increased.[17] In the latter case, at a constant 55% surfactant, the diameter of rod-aggregates decreases with increased ethanol content from 45 to 38 Å (assuming the aggregates contain only the surfactant), and the area per headgroup increases from 53 to about 90 Å.[21] The decrease of 7 Å in the cell constant is comparable to that seen in the water:methanol:silica system for HPS. Thus, we have shown that cosolvents can be used to tune the degree of aggregation and the aggregate diameter of the surfactant templates.

2. The Ordered Hexagonally Packed Silica Existence Region (o-HER). The o-HER was examined for each of the cosolvents in Table 1 by varying *r* (Figure 8). For cosolvents with dielectric constants (ϵ) less than 10, the existence region is quite small ($0\% \leq r < 20\%$), except for tetraglyme. Several of these systems phase separate prior to the addition of TMOS, which limits the formation of periodic mesophases from mixed water:nonpolar solvent systems to substantially aqueous environments.

For methylene chloride and THF (Figure 4), the structure of the product changes from o-H to L rather than o-H to d-H as in other systems (see Table 1); the changes occur at $r \approx 2\%$ and $r \approx 18\%$. For diethyl ether the structure of the silica/surfactant mesophases changes from o-H to C to L, paralleling the classical E → Q → D evolution for LC phases;[12] the changes occur at $r = 10\%$ and $r = 12\%$, respectively. Direct transformation from o-H to L is seen for an $r = 20\%$ THF sample (Figure 4).

The transformation from L to H has been observed previously.[24] The transformation can be understood by applying the simple theory of micellar structure that was developed by Israelachvili et al.[33] based on the geometry of micellar shapes and the space occupied by the hydrophilic and hydrophobic groups of the molecule. The critical packing parameter (CPP) is defined as $V_H/$

(33) Israelachvili, J. N.; Mitchell, D. J.; Ninham, B. W. *J. Chem. Soc., Faraday Trans. 2* **1976**, *72*, 1527.

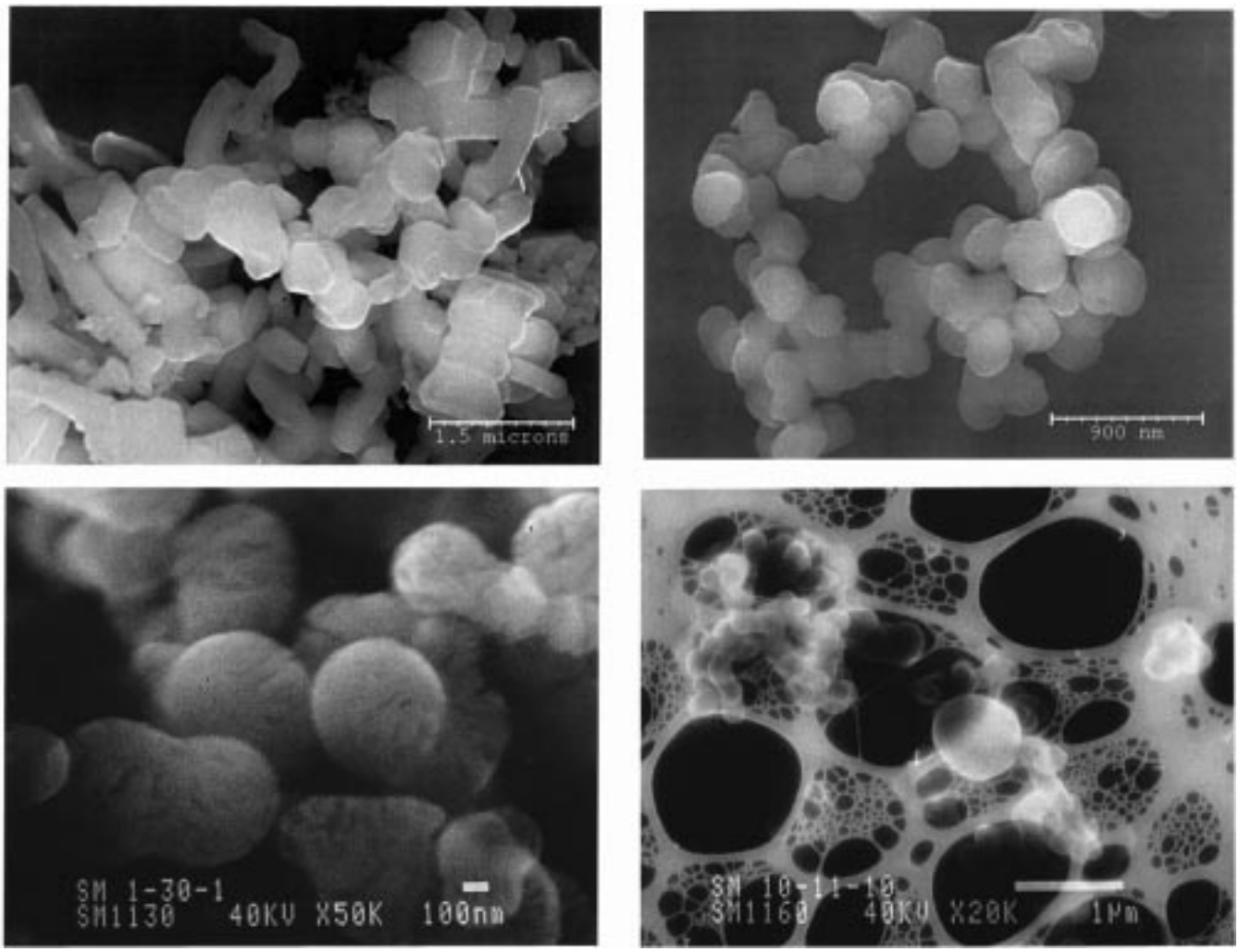

Figure 17. Scanning electron micrographs of samples prepared in pure water (top left), 25% methanol (top right), $r = 20\%$ THF (lower left), and $r = 90\%$ formamide (lower right).

$a_o l_c$, where V_H is the volume of the hydrophobic portion of the molecules, a_o is the optimum headgroup area, and l_c is typically: $l_c \leq 1.5 + 1.265n$ Å, where n is the number of carbon atoms in the chain. The exact value of l_c depends on the extension of the chain. The aggregate structure depends on the value of the CPP: the larger the CCP, the less curvature in the aggregate. In the case of the low dielectric constant cosolvents, over time some of the cosolvent diffuses into the tail region (Figure 12), which increases V_H, which in turn increases the CCP and favors structures with a lower curvature and headgroup volumes (i.e. L over H).

The extensive o-HER for the polyether tetraglyme is anomalous among low dielectric constant cosolvents. Tetraglyme is a large polyether molecule that contains five oxygen atoms. We postulate that in water the oxygens can interact with hydrogen atoms on water to form a reasonably well structured network. The structure of the solvent system presumably enhances the formation of spherical micellar aggregates and disfavors the dissolution of CTAB into free surfactant molecules. The formation of spherical micelles in turn favors the formation of o-H rather than d-H products (see below). The miscibility of the cosolvent and water at high values of r presumably leads to the large observed o-HER. The length of tetraglyme likely prevents its solubilization deep in the core of the micelle, which prevents the formation of lamellar mesophases.

For cosolvents with $10 < \epsilon \leq 24$, the o-HER is $0\% \leq r < \sim 50\%$ (Figure 8). In these cases there is an evolution from o-H to d-H at high values of r. The d-H phase can persist at relatively high values of r (up to 90% for methanol). It is quite interesting to note that for methanol and ethanol the o-HER is $r = 0-60\%$ and $r = 0-40\%$, respectively, but in the simple water/alcohol/CTAB system, the E liquid crystalline phase does not exist for methanol concentrations greater than 25% or ethanol concentrations greater than 20%.[17] The behavior of the amphiphile in the presence of silica underscores the cooperative nature of the organization of the system into an ordered LC-type (SLC) structure.

For highly polar cosolvents with $\epsilon > 24$, the existence region is from $r = 0\%$ to $r > 90\%$ (Figure 8). The large o-HER for these polar solvents is not particularly surprising especially for the protic donor solvents glycerol, ethylene glycol, formamide, and *N*-methylformamide as lyotropic LC phases exist in these solvents.[11−16] The o-HER follows the sequence formamide > *N*-methylformamide > ethylene glycol ≫ glycerol, which is different from the existence regions of liquid crystals formamide ≫ glycerol > ethylene glycol > *N*-methylformamide.[11] Although the comparison be-

tween phase fields is not direct, it is again clear that silica affects LC behavior of the surfactant.

3. Nonaqueous Synthesis. At $r > 90\%$ the water-to-silicon ratio (h) is < 9.0, and water begins to serve mostly as a reagent. o-H phases have been made with $r = 93\%$ for formamide (Figure 2). d-H phases have been synthesized for glycerol and methanol with r equal to at least 90%. d-H phases have been made for $r > 93\%$ in the ethylene glycol ($h = 3.9$; $r = 97\%$) and formamide systems ($h = 5.2$; $r = 96\%$, diffraction peak at $d \gg 33$ Å; Figure 2). In these cases the syntheses can be considered nonaqueous, as the water acts almost solely as a reagent.

As the existence of LC phases in pure ethylene glycol[11,12,16] and formamide[11−15] is well documented, we assume that the maximum value of r for the formation of HPS is thus substantially limited by the inorganic chemistry. It has been shown that *condensation between* polynuclear species (double four rings) is not necessary to form HPS,[9] but it has been postulated that the presence of some of these multicharged polynuclear species (oligomers) is necessary to the assembly process.[24] Thus there must be enough water present to enable hydrolysis of and some condensation TMOS monomers.

Finally, at very high values of r, transparent chemical gels form over several hours. In these cases, the surfactant no longer acts as a chemical dipole and/or there is simply not enough water to rapidly form suitable silicate oligomers, thus chemical gels that contain entrapped surfactant form rather than HPS.

It is useful to consider why the some high dielectric constant cosolvents, that is, acetonitrile and *N*-methylformamide, do not support mesophase formation in substantially nonaqueous environments (Figure 8). For acetonitrile the solvent phase-separates at $r \gg 50\%$, which limits h to ~65 for HPS formed out of homogeneous solution. For *N*-methylformamide the dielectric constant is very high. The effective charge screening provided by the solvent may destabilize the inorganic−organic salt formed in mesophases and may thus frustrate the transformation from surfactant plus silica to an ordered liquid crystalline mesophase. We also note the absence of E LC phases in pure *N*-methylformamide, which may disfavor HPS at high concentrations.[11]

4. Effect on Micellization and Product Periodicity. The intensity above background measured with static light scattering decreases as r increases for all of the polar cosolvents shown in Figure 9. The decrease in scattered intensity indicates a decrease in degree of aggregation and/or a decrease in aggregate size. We have previously shown that for the water:methanol system the decrease in scattered intensity corresponds to both.[26] At $\Delta I = 0$ it is certain that the aggregates are absent or are so small that they cannot be detected by light scattering.

In the other cosolvent systems, we also assume that the *cmc* is approximately equal to the surfactant concentration (2 wt %) at the value of r for which $\Delta I = 0$. Thus, the *cmc* increases from about 0.036 wt % in pure water to 2.0 wt % at approximately $r = 40\%$ for ethanol, at $r = 60\%$ for methanol, and at $r = 90\%$ for formamide.

If we compare the maximum value of r in Figure 8 with the value of r at $\Delta I = 0$ in Figure 9, we see that the o-H to d-H transformation occurs at approximately the same value of r at which there are no longer aggregates detectable by SLS in the simple water/cosolvent/CTAB system. For example, for methanol the r values for o-H to d-H and $\Delta I = 0$ are 70% and 60%, for ethanol are 40% and 40%, and for formamide are 93% and 90%. This implies that the long-range 2-d hexagonal order is quite sensitive to the micellization of the surfactant in the precursor solutions. Assembly from micellized surfactant presumably involves interfacial templating of surfactant assemblies and small, *in situ*-generated silicate species on a supramolecular length scale.[9] In contrast, assembly from nonmicellized surfactant lacks spatially extended surfactant arrays, at least initially, and is probably limited to interfacial interactions on a molecular length scale. It is this difference in spatial extent of interfacial templating we believe that leads to materials which exhibit long-range (o-H) versus short-range order (d-H).

Silica Chemistry and Kinetics. Cosolvents are also expected to affect the chemistry of silica hydrolysis and condensation. For o-H products the process occurs so rapidly (in all cases physical gels form in 10 s or less) that it is difficult to determine accurately the effects of cosolvents on the formation kinetics. We would expect protic solvents to slow the kinetics of TMOS hydrolysis and condensation slightly, which should slow the evolution of charged silicate oligomers;[22] however, we are unable to unambiguously show this owing to the short time scale of product formation. For d-H products, the formation time can be increased as much as 4-fold (for $r = 90\%$ methanol, for example), but for d-H products the water-to-silicon ratio is typically low (as low as 4), so it is difficult to deconvolute the effects of a reduced water/silicon ratio with those of the solvent without a much more detailed study.

Finally, we point out that the silica/surfactant mesophases are inherently transient, as the silica condensation continues for many days after formation if the product is aged in the mother liquor. For example, with $r = 25\%$ methanol the Q^3/Q^4 ratio decreases from ~2.1 10 min after formation to ~1.1 after 7 days.[26] The cosolvent/water ratio undoubtedly influences the condensation rate during the aging process, especially for protic solvents that can interact with hydroxide ions and reduce their nucleophilicity (see reaction 3). The condensation in low water environments is, however, sufficient to prevent collapse of the framework upon calcination even at relatively low water-to-silica ratios (Figures 13 and 14).

6. Cell Constant Control. In addition to regulating the water concentration and structure type, cosolvents can be used to continuously tune the cell constant of the mesoporous products (Figure 10). Protic cosolvents, such as methanol, *N*-methylformamide, formamide, glycerol, ethylene glycol, and ethanol, which have the ability to hydrogen bond, shrink the mesophase unit cell as their concentration increases, whereas aprotic cosolvents, such as acetonitrile, acetone, and tetraglyme, expand the mesophase unit cell as their concentration increases (Figures 1 and 11).

The cosolvent−solvent and cosolvent−surfactant interactions are undoubtedly complex, but the different effect of protic versus aprotic cosolvents (Figure 11) may lie in their locus of solubilization within a micelle. Protic cosolvents are believed to be solubilized nearer the headgroups of the surfactant molecules, in proximity to the polar solvent.[20] Protic solvents thus have the ability to reduce repulsive headgroup interactions and reduce micelle diameter. Aprotic cosolvents are believed to be solubilized deeper within the micelle where they tend to expand the hydrophobic volume and increase the micelle size.[20] Regardless of the microscopic nature of the effect, cosolvents can be used to continuously tune the unit cell constant (and pore diameter)[26] of the mesophases.

7. Mixed-Metal Frameworks. Another advantage of the cosolvent approach to mesoporous oxides is that two or more alkoxides can be mixed and prehydrolyzed in an nonaqueous solvent, which can, by matching hydrolysis rates of the alkoxides, lead to a solution that contains heteroatomic M−O−M′ bonds. This can lead to an as-made mesophase product with a homogeneous distribution of dopant ions in the framework (Figure 16).

A similar approach was used by Kim et al.[18] who used a 10% CTACl in formamide solution to dissolve titanium *n*-butoxide and then added precipitated silica to this followed by aqueous sources of dissolved silica. In their case mesophases were formed from $r = 86\%$, $h = 8.6$, [Si] ≈ 0.92 M solutions.

8. Effect on Microstructure. Figure 17a−d shows that the cosolvents have a dramatic affect the maximum diameter, dispersity, and shape of grains. Their use leads to smaller primary particles that have greater curvature than samples made in pure water. Figure 17a shows that the $r = 0\%$ sample has well faceted crystallites that comprise truncated triangular plates and 1−1.5 mm by 0.6 mm wormlike tubules. The HPS gels made in the presence of cosolvents tend to form as aggregated submicron spherical or ellipsoidal particles. For example, Figure 17b shows the an $r = 25\%$ methanol preparation in which consists of aggregated 300−400 nm spherical or ellipsoidal particles. Figure 17c shows the aggregated submicron spherical particles for the a lamellar $r = 20\%$ sample. Figure 17d shows that a large dispersity occurs for $r = 90\%$ formamide samples. Table 2 summarizes the effect of cosolvents on HPS microstructure.

The faceted morphology observed for $r = 0\%$ samples was reported in seminal articles on MCM-41.[1,2] The reason for the greater curvature observed for solvents prepared in the presence of cosolvents is difficult to explain without more extensive investigation, but we note that from the LC literature, the spatial extent of rodlike micelles is much less in nonaqueous solvent systems than in water.[14] In fact the spatial extent of the rods in the E LC phase with nonaqueous solvents does not approach that for the aqueous rodlike micelles until near the E → Q phase boundary. The smaller spatial extent of the LC phases may be related to the smaller, highly curved grains observed in the HPS materials.

Table 2. Effect of Cosolvents on Microstructure

cosolvent	*r* (%)	grain size (nm)	grain shape[d]
water	-	150−500	E
tetrahydrofuran	20	150−600	E/S
tetrhydrofuran[a]	10	150−600	E/S
acetone	40	300−600	S
isopropanol	15	200−750	E
methanol	25	150−500	E/S
methanol[b]	25	250−500	E
methanol	40	150−700	E
formamide	90	200−100	E/S
formamide[c]	50	25−100	S
ethylene glycol[c]	50	10−50	S

[a] Made with a 2-butanol:CTAB ratio of 2.7:1. [b] Made at 10 °C and 50 °C with a 2-butanol:CTAB ratio of 2.7:1. [c] Thin film made with ammonia gas rather than NaOH as the catalyst. [d] E = ellipsoidal; S = spherical.

Conclusions

Silica/surfactant mesophases that have ordered hexagonal (o-H), disordered hexagonal (d-H), lamellar (L), and cubic (C) structures can be formed in mixed water: cosolvent systems. o-H structures form in all systems that support E type liquid crystalline (LC) phases in the simple CTAB/solvent system, and also form in the water/NMF system, for which the pure NMF system supports only D type LC phases. Cosolvents allow the cell size and pore diameter to be continuously tuned over ∼5 Å: protic solvents decrease the cell constant owing to hydrogen bonding with the continuous phase and siting near the headgroups; aprotic solvents increase the cell constant owing to solubilization deeper within micellar structure. Polar cosolvents tend to decrease the aggregation and/or aggregate size of CTAB, and lead to highly porous disordered hexagonally packed silica (d-H) when the concentration of CTAB is less than *cmc*. Polar solvents that support LC phases also support substantially nonaqueous synthesis of HPS. Low dielectric constant solvents lead to swollen o-H products at low concentrations and, by increasing the hydrophobic volume, to cubic and lamellar products at higher concentrations. Mixed-metal frameworks can also be formed in a controllable manner using cosolvents. Cosolvents have a dramatic affect on microstructure and tend to make particles with much greater curvature and smaller size than purely aqueous systems, perhaps owing to the propensity of the surfactant molecules to form less extended LC arrays.

Acknowledgment. We thank Ralph Hunkins for the ^{27}Al NMR. This work was funded by the United States Department of Energy under Contract No. DE-AC04-94AL85000.

CM9704600